We are IntechOpen,
the world's leading publisher of
Open Access books
Built by scientists, for scientists

6,900
Open access books available

186,000
International authors and editors

200M
Downloads

Our authors are among the

154
Countries delivered to

TOP 1%
most cited scientists

12.2%
Contributors from top 500 universities

CLARIVATE ANALYTICS
BOOK CITATION INDEX
INDEXED

WEB OF SCIENCE™

Selection of our books indexed in the Book Citation Index
in Web of Science™ Core Collection (BKCI)

Interested in publishing with us?
Contact book.department@intechopen.com

Quasi-optical Systems Based on Periodic Structures

Gennadij Vorobjov[1], Yulya Shulga[1] and Vitaliy Zhurbenko[2]
[1]Sumy State University, Ukraine
[2] Technical University of Denmark,
[1]Ukraine
[2]Denmark

1. Introduction

Open resonators and open waveguides are widely used in millimeter and submillimeter wave electronics because they provide lower loss and higher Q-factor in comparison to the standard closed structures [Valitov et al., 1969; Shestopalov, 1985; Weinstein, 1966, 1995] . Examples of high performance measurement equipment employing open resonators (based on spherical or semispherical mirrors) include resonant wave meters, reference oscillators, systems for measurement of intrinsic electromagnetic properties of dielectric materials, and others [Valitov et al, 1969; Milovanov and Sobenin, 1980; Valitov and Makarenko, 1984]. Semispherical and spherocylindrical open resonators in combination with reflective diffraction gratings are used in various diffraction radiation oscillators [Shestopalov, 1976, 1985, 1991] providing higher frequency stability and output power in comparison to the standard devices such as traveling-wave tubes, klystrons, and magnetrons. Open resonators with echelette-type corner mirrors have been chosen as the basis for highly efficient Gunn and IMPATT diode oscillators. Quasi-optical resonators of such devices adopt reactive reflection and transmission-type schemes [Sukhoruchko et al., 2003]. Open resonators has found a wide practical application in relativistic electronics. Several types of oscillators and amplifiers have been created on their basis [Balakirev et al., 1993]. It has been demonstrated by [Weinstein and Solntsev, 1973] that Smith-Purcell effect (diffraction radiation) can be used to build an amplifier based on an open waveguide.

The constantly growing interest in the implementation of millimeter and submillimeter wave radiation in different areas of science and technology puts forward demands for components with high performance and flexible functionality. One of the most promising strategies for the development of such components is to modify their electromagnetic structure in order to increase operating frequency band and improve efficiency of interaction between the electron beam and electromagnetic wave. Following this strategy, several new approaches have been proposed based on modification of open coupled electromagnetic structures such as coupled open resonators [Shestopalov, 1991], open waveguides [Weinstein, 1995; Weinstein and Solntsev, 1973], open resonators with dispersion elements [Marshall et al., 1998], as well as the metal-dielectric structures [Shestopalov, 1991] which are particularly useful for electromagnetic wave excitation

employing Cherenkov effect. Unfortunately, the practical realization of the proposed structures is a rather difficult task because of complicated electromagnetic analysis and a lack of systematic approach.

The objective of this chapter is to perform a comparative analysis of classical quasi-optical structures and their new modifications. The strategies for further development of these structures will be discussed based on the performed analysis.

The chapter starts with a description of basic properties of a classical regular open resonator as a basis for new modified millimeter and submillimeter wave coupled resonant structures. The properties of open resonators and open waveguides based on periodic metal and metal-dielectric discontinuities excited by both the electron beam and the surface wave of the dielectric waveguide are considered.

2. The coupled quasi-optical systems based on open resonators

This section is dedicated to the analysis of simple (regular) resonant systems and coupled quasi-optical systems based on periodic metal and metal-dielectric structures such as open resonators with diffraction grating, coupled open resonators and resonators with layered metal-dielectric structures.

2.1 The main properties of classical quasi-optical resonators

A classical quasi-optical resonator consists of two-mirrors. In the simplest case considered here, the open resonator contains two opposing flat infinitely thin parallel aligned disks. This system of mirrors is referred as plane-parallel resonator and known from optics as the main part of Fabry-Perot interferometer.

The plane-parallel resonators exhibit a number of valuable properties: sparse spectrum of resonant frequencies, homogeneous field along the symmetry axis of the resonator and the wavelength in the resonator is slightly different from the wavelength in the free space.

While simple, this arrangement is rarely used in practice due to the difficulty of alignment, comparatively large size, and insufficient mode separation. Therefore the resonators based on the reflectors with quadratic phase correction are more promising in the millimeter and submillimeter wave range. These type of resonators are referred as confocal resonators and contain spherical mirrors. These resonators exhibit a better spectral resolution in comparison to the plane-parallel resonators. Besides, confocal resonators are less sensitive to misalignment. The resonator with spherical reflectors typically exhibits lower power loss per one propagation in comparison to the open resonator with plane mirrors having the same aperture. The other important advantage is the large separation between the fundamental and the higher order modes TEM_{mnq}, where $m, n = 0, 1, 2,...$ is the number of half-waves in transverse direction and q is the longitudinal index which corresponds to the number of half-waves in the direction of propagation. For the resonator with spherical mirrors the resonance distances or the resonance wavelengths of the oscillation modes should comply with the following condition:

$$\frac{2H}{\lambda} = q + \frac{1}{\pi}(m + 2n + 1)\arccos\sqrt{g_1 g_2} \,, \tag{1}$$

where H is the distance between the mirrors; λ is the wavelength in the open resonator; $g_1 = 1 - \dfrac{H}{R_1}$; $g_2 = 1 - \dfrac{H}{R_2}$; R_1, R_2 are the curvature radii of the mirrors.

Limiting the size of resonator's apertures results in radiation loss and has negligible effect on the field distribution in the open resonator. Therefore the field must be concentrated close to the center of the mirror in order to reduce the losses. This, in turn, restricts the choice of ratio between the radius of the curved mirrors and the distance between them. In order to construct resonators with the field concentrated close to the center of the mirror, the distance between the mirrors must be selected within the following intervals:

$$0 < g_1 g_2 < 1. \tag{2}$$

This expression is known as the condition of stability of the resonator with quadratic correction; g_1, g_2 are the parameters that depend on geometry of the resonator.

The behavior of oscillations in plane-parallel and spherical-mirror resonators is quite different. The field distribution in the plane-parallel resonator mostly depends on the dimensions of the plane plates, while field distribution in the resonator with spherical mirrors is mostly determined by their radius and the ratio of the distance between mirrors and the radius, $\dfrac{H}{R}$.

The semi-spherical resonators which consist of a plane and a spherical mirror have also received a great deal of interest in microwave and millimeter-wave applications. It is known that the fundamental modes of the semi-spherical resonator are represented by the azimuthal oscillations TEM_{m0q} . If the field spot on the plane mirror is considerably smaller than its diameter then the semi-spherical resonators can be substituted by the equivalent resonators with two spherical mirrors having doubled distance between them. The distribution of amplitudes in both cases is identical to a high degree of accuracy. The Q-factor of the semi-spherical resonator depends on diffraction losses at the edges of the plane and the spherical mirrors, ohmic losses in the mirrors, the coupling losses and the losses related to attenuation in the medium.

2.2 Resonators with periodic metal grating

The plane-parallel mirror of the semi-spherical resonator can be substituted by a diffraction grating as it is shown in Fig. 1. Such an electrodynamic structure is often used in diffraction radiation oscillators - orotrons [Shestopalov, 1976, 1991; Marshall et al., 1998; Ginzburg et al., 2000; Bratman et al., 2002; Rusin et al., 2002].

The orotron's operation principle is based on the diffraction radiation effect caused by the electron beam propagating above the diffraction grating of the open resonator. The electron beam interacts with the incident field diffracted from the grating which results in oscillation and amplification of the electromagnetic signal. Therefore, the orotron's output characteristics are strictly defined by the properties of the implemented open resonator. The periodic structure in the open resonator of the orotron considerably changes the characteristics of the previously described classical resonant quasi-optical structures. The substitution of the plane mirror by a diffraction grating considerably increases the total loss resulting in the Q-factor degradation by almost four times. The decrease of the Q-factor

occurs as the result of additional losses, which are originated from a power leakage of the waveguide waves propagating along the grooves to the edges of the mirror where the reflection coefficient is not equal to one.
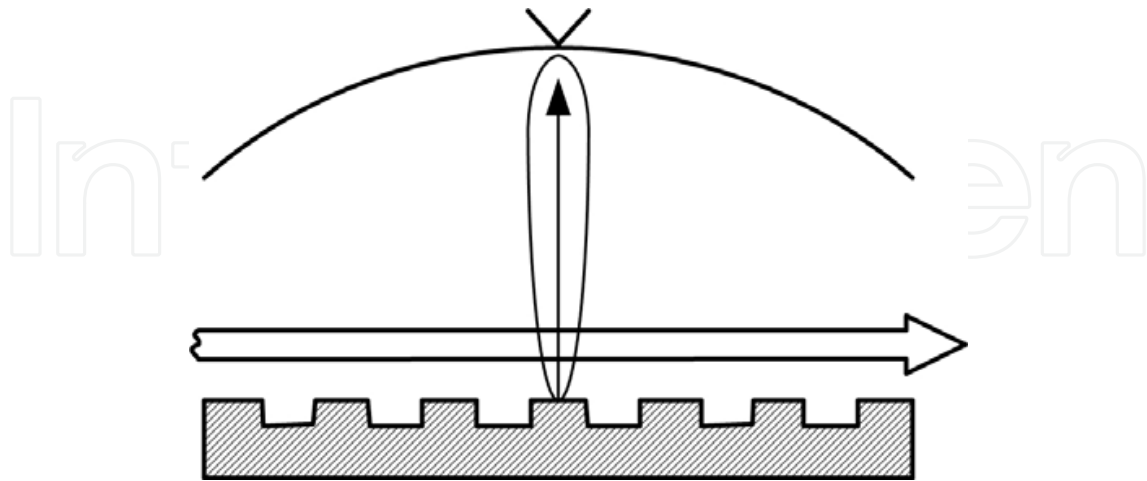

Fig. 1. Semispherical open resonator with diffraction grating

To overcome this drawback, a semi-spherical resonator where only the central part of the plane mirror was covered with the diffraction grating, has been proposed [Shestopalov, 1976, 1991]. This resonator has a wider distance between the oscillation frequencies. The achieved radiation loss depends on the parameters and the position of the grating. The width of the grating defines the number of the oscillation modes excited in the open resonator and the frequency of the higher order resonances. Losses in the open resonator are greatly dependent on the ratio between the period of the grating and the wavelength. The maximally achieved Q-factor of the resonator also greatly depends on the groove depths of the reflective grating oscillations could be varied by several times.

The fundamental mode of the semi-spherical resonator with a local diffraction grating is TEM_{20q}. The research in [Shestopalov, 1976, 1991] proved that the perturbation caused by the grating is insignificant in such a system if the minimum of the field distribution is above the boundary between the grating and the mirror. This is the case when the width of the diffraction grating is larger or equal than the width of the main lobe in TEM_{20q} oscillation mode.

Corner-echelette open resonators are widely used for realization of semiconductor sources in the microwave and millimeter-wave range. For example, modifications of quasi-optical reflection and transmission-type solid-state pump oscillators with spherical-corner-echelette open resonator have been shown in [Belous et al., 2003]. As shown in [Sukhoruchko et al., 2003], the corner-echelette resonator has the following properties: the degree of sparseness of the spectrum is lower than for the resonator with plane echelette mirror; however, the spectrum contains the oscillation modes with extremely high Q-factor, which are known as the quasi-fundamental oscillation modes; the field of the quasi-fundamental oscillation modes is concentrated around the axis of the open resonator resulting in a larger power density in comparison to the fundamental and higher order oscillation modes; the field distribution close to the surface of the corner-echelette mirror transforms and near the center of the resonator becomes similar to the field in a rectangular waveguide; corner-echelette mirror can be considered as a multi-step impedance transformer.

2.3 Coupled open resonators

The work by [Shestopalov, 1991] is dedicated to the diffraction radiation devices employing coupled open resonators. The coupled resonators have an advantage of providing a wider operating frequency range in comparison to the single resonator structures. The coupling between open resonators can be realized either by means of the field diffracted at the edges of the mirrors using series positioning of the resonators (Fig. 2a) or the field diffracted on a metal-strip grating using parallel connection of open resonators (Fig. 2b) with respect to the axis of the distributed excitation source. In the electron devices, the electron beam is such a source. In case of experimental modeling of diffraction radiation it is the surface wave of the single-mode dielectric waveguide.
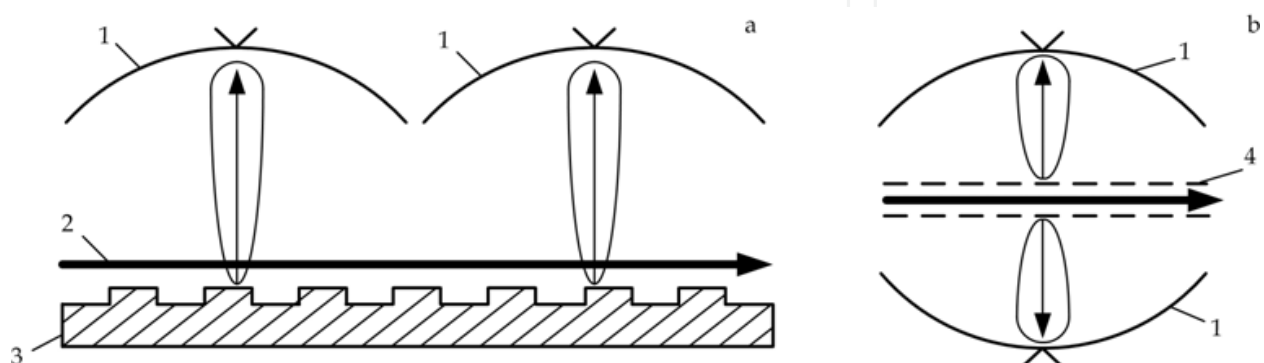

Fig. 2. Electrodynamic systems based on coupled open resonators: a – series connection of open resonators; b – parallel connection of open resonators

The system of series open resonators is, in the case shown in Fig. 2a, consists of two semi-spherical resonators with the common plane mirror realized as a reflective diffraction grating. In the parallel coupling case (Fig. 2b), a two-layer metal-strip diffraction grating is placed between the spherical mirrors.

Systems of coupled open resonators consist of spherical mirrors **1** with the radius R=60 mm and aperture A=55 mm reduced to 35 mm along the axis of the dielectric waveguide **2**. The lower plane mirror **3** of the system shown in Fig. 2a is either a reflective or semitransparent diffraction grating and serves as a common mirror for the first and the second open resonator. In the system with parallel open resonators, plane mirrors **4** with semitransparent diffraction gratings in their central sections were placed between spherical mirrors **1**.

Parameters of the gratings are chosen to ensure the operation at a frequency $f_0 = 46\ GHz$. These gratings transform the surface wave of the dielectric waveguide into a free space wave propagating normal to the surface of the grating [Shestopalov, 1976]. The energy is coupled out from the system through the coupling slots in the spherical mirrors. The signals are then fed to a detector and measured using a standard measurement equipment [Shestopalov, 1976, 1991].

The described coupled resonators have been analyzed with regard to their spectra and resonance characteristics of oscillation. The measured characteristics of the equivalent single hemispherical and spherical open resonators have been used as a reference.

Fig. 3 shows the resonant frequencies versus the distance between the mirrors (H) in the system with coupling through the diffraction field (Fig. 2a) and in a reference hemispherical open resonator. The data presented in Fig. 3 characterizes the capability of the considered resonance system to support a limited number of TEM_{mnq} oscillation modes.
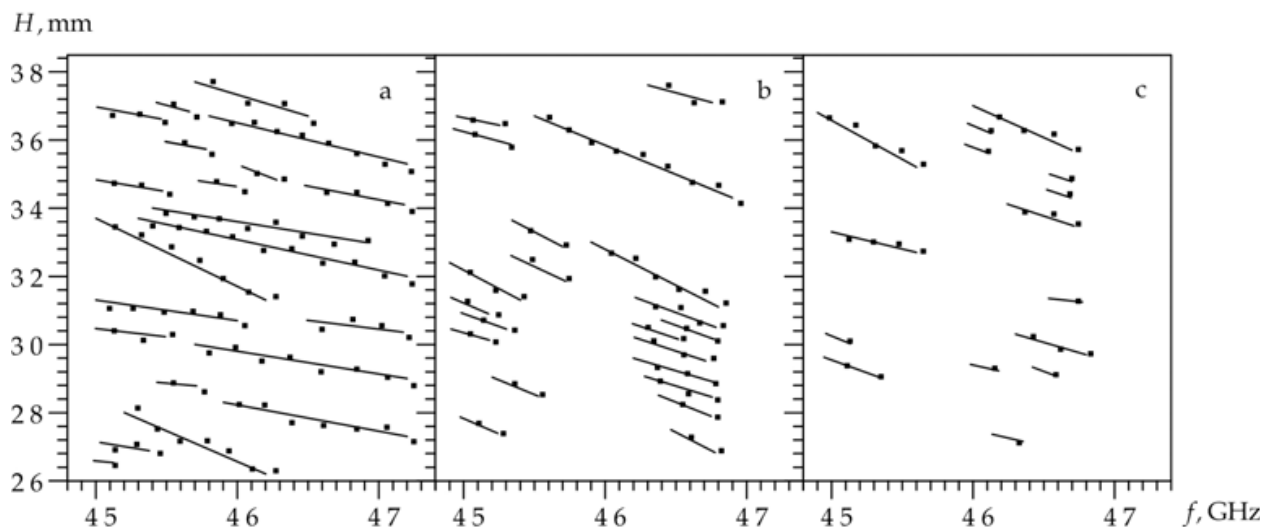
H, mm

Fig. 3. Spectra of resonant frequencies of (a) a hemispherical resonator and (b, c) a diffraction-coupled resonators with (b) reflective and (c) strip diffraction gratings.

The data in Fig. 3a shows that for the hemispherical open resonator, the fundamental TEM_{00q} modes exist in the entire frequency range $f = 45 - 47\,GHz$ while changing the distance between the mirrors. The implementation of a dispersive element such as the reflective diffraction grating in the open resonator allows for the modes with transverse indices m and n. The TEM_{20q} oscillation mode is usually a fundamental mode for such resonators [Shestopalov, 1991]. In addition to the fundamental modes, depending on the parameters of the open resonator and the diffraction grating, the other types of higher order oscillations (e.g., TEM_{02q}) occur influencing the coupling between the two open resonators through the diffraction fields.

Figure 3b shows the resonances of two coupled open resonators tuned to a frequency f=46 GHz. As can be seen from these spectra, the second hemispherical open resonator is excited at the edge points of the frequency band in the interval H=27–33 mm. There are no oscillations around the resonance frequency of the open resonator, which is due to the minimum amplitude of the diffraction field in a case when the diffraction-grating–dielectric-waveguide system emits radiation along the normal. Detuning from the frequency f_0 in the interval $\Delta f \approx \pm 1\,GHz$ leads to the deviation of the main lobe direction from the normal, which increases the intensity of the diffraction field and, consequently, leads to the excitation of the second resonator at the edges of the frequency range. As the distance H increases, the coupling between the resonators becomes stronger reaching its maximum magnitude when the distances between the mirrors are equal to each other. In this case, oscillations in the second open resonator arise even at a frequency $f \approx 46\,GHz$.

Coupled open resonators with a strip grating at the center of the common plane mirror (Fig. 2b) exhibit similar properties. The decrease in the number of oscillation modes in such a system (Fig. 3c) is due to the selective properties of the employed diffraction grating [Shestopalov, 1991]: the intensity of radiation emitted from the volume of the open resonator to free space through the diffraction grating reaches its maximum at $H \approx (\lambda/4)(2N+1)$, while the accumulation of energy inside the volume of the open resonator appears at values $H \approx (\lambda N)/2$, where λ is the radiated wavelength, N = 1, 2, … . The coupling in open

resonators reaches its maximum when the distances between the resonators are approximately equal to each other, i.e., when the resonators are tuned to close frequencies. The typical response of the previously described coupled open resonators is presented in Fig. 4. Here P/P_{max} is the power in the open resonators normalized to the maximum power P_{max}. The resonance curve of a hemispherical open resonator is shown for comparison (curve 1) in the same figure. As can be seen from the presented data, the transmission band of coupled open resonators measured at the level of $0{,}5P_{max}$ increases by a factor of nearly two, resulting in $\Delta f \approx 250\,MHz$. The resonance curves corresponding to coupled open resonators with reflective and strip diffraction gratings virtually coincide with each other under these conditions, which indicates the existence of efficient coupling in these systems through the diffraction of the fields at the periphery of the mirrors.
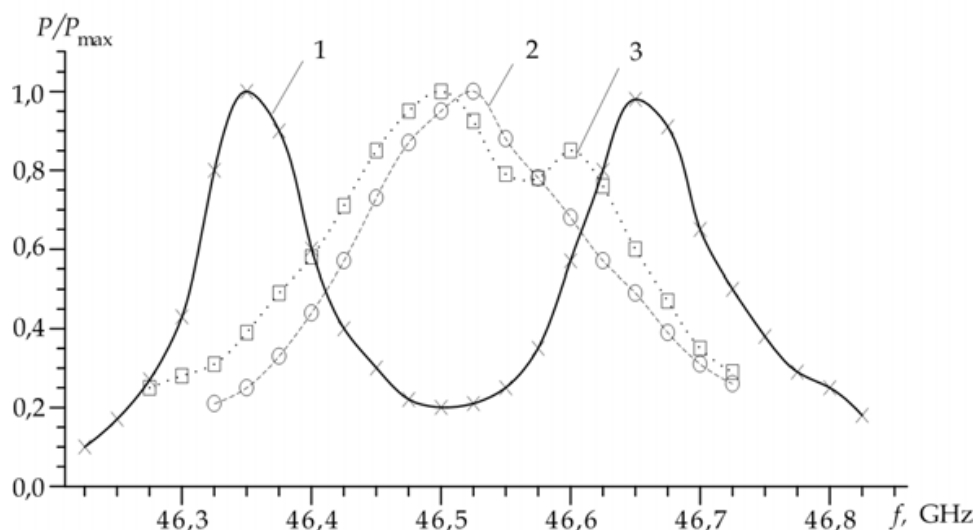

Fig. 4. Response of (1) a hemispherical open resonator and (2, 3) coupled open resonators with (2) metal-strip and (3) reflective diffraction gratings

The open resonator with spherical mirrors, which is a basis for the second scheme of coupled resonators (Fig. 2b) supports similar to the case of the hemispherical open resonators fundamental TEM_{00q} modes. This follows from the analysis of the achieved resonance frequencies. The field distribution in an open resonator with spherical mirrors is the same as in the hemispherical open resonator [Shestopalov, 1976]. However, the distance between the resonance frequencies in the open resonator with spherical mirrors is two times smaller than in a hemispherical open resonator. Inserting an additional plane mirror with a strip diffraction grating in a spherical open resonator will result in the spectrum of the coupled system similar to the spectrum of the hemispherical open resonator (Fig. 3a). The metal-strip diffraction gratings couple two hemi-spherical open resonators simultaneously filtering out the angular spectrum of plane waves excited in the system. Consequently, the variation of the position of these diffraction gratings in the volume of the resonator with respect to the spherical mirrors changes the spatial distribution of the fields corresponding to the oscillation modes excited in the considered system of coupled open resonators. Similar to the hemispherical open resonator with a reflective diffraction grating, TEM_{20q} and TEM_{02q} oscillation modes, as well as the higher order oscillation modes arise due to introducing a coupling element such as a double-layer diffraction grating.

The measured data for the resonance curves of coupled open resonators indicates that the achieved bandwidth of the system becomes much broader when the open resonators are tuned to close frequencies rather than in the case when the resonators are coupled through the diffracted fields. Fig. 5 presents the response of the open resonators coupled through a strip diffraction grating and for the open resonator with spherical mirrors. The achieved bandwidth of the coupled system was observed within the range $f = 44,5 \div 49,5\,GHz$ for equal distances of spherical mirrors from the planes of the coupling element with a total distance between the spherical mirrors equal to H=31 mm. The achieved bandwidth measured at the $0,5P_{\max}$ power level is equal to $\Delta f \approx 1,3\,GHz$. The narrowing of the transmission band of coupled open resonators observed in the higher frequency band (f=48,5 GHz) is due to the deviation of the radiation pattern for the diffraction grating–dielectric waveguide system from the normal and, consequently, the decrease in the coupling coefficient between the resonators.
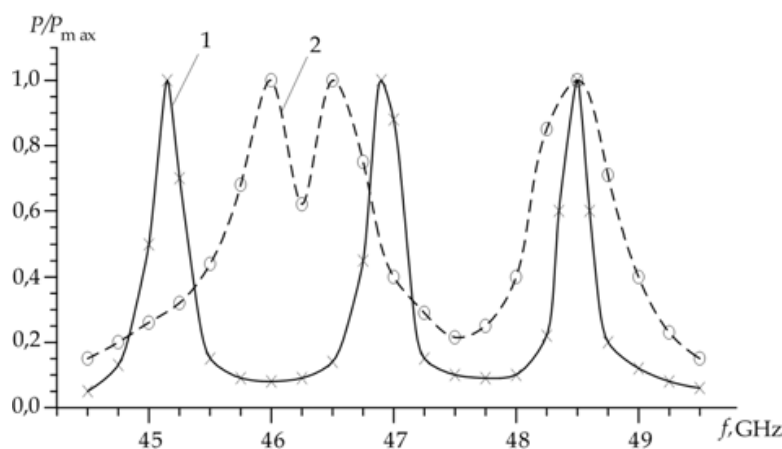

Fig. 5. Response of (1) the spherical open resonator and (2) the system of resonators coupled through semitransparent diffraction gratings.

Analysis of the achieved bandwidth Δf for the single resonator and coupled systems shows that the maximum bandwidth in systems with comparable H can be achieved when two open resonators are coupled through a strip diffraction grating. The bandwidth of the system with parallel open resonators is almost five times wider than the bandwidth of the system with series open resonators. It should be noted that the Q-factor of the coupled open resonators is of the same order as the Q-factor of the single open resonators. Therefore the open resonators coupled through the strip diffraction grating are preferable for systems requiring wideband operation. Such resonators also provide a reduced size of the system along the electron beam propagation axis.

2.4 Open resonators with metal-dielectric structures
Coupled systems based on open resonators and open waveguides with metal-dielectric structures allow to realize different modes of energy transformation depending on parameters of the electromagnetic system [Shestopalov, 1991].
The simplest open resonator employing a metal-dielectric slab is shown in Fig. 6a. It consists of a metal plane and a dielectric slab with a planar metallic diffraction grating on its surface.

ε is the permittivity of the dielectric. The source of electromagnetic energy is distributed along the grating. It excites various spatial harmonics of Cherenkov diffraction radiation of order $n = 0, \pm 1, \pm 2,...$ and the power density S_n, which depends on the parameters of the structure. Fig. 6a demonstrates the excitation of Cherenkov ($S_{0\varepsilon}$) and minus first diffraction ($S_{-1\varepsilon}$) harmonics in the dielectric as well as minus first diffraction harmonic (S_{-1v}) in open volume, which can be reflected back by a metal plane and fed to the metal-dielectric channel. A number of numerical and experimental methods for simulation of different excitation modes of Cherenkov diffraction radiation has been developed [Vorobyov et al., 1997, 2007]. They allow to determine the quantitative relation between the power densities of spatial harmonics in the structure as well as to optimize and tune their parameters.
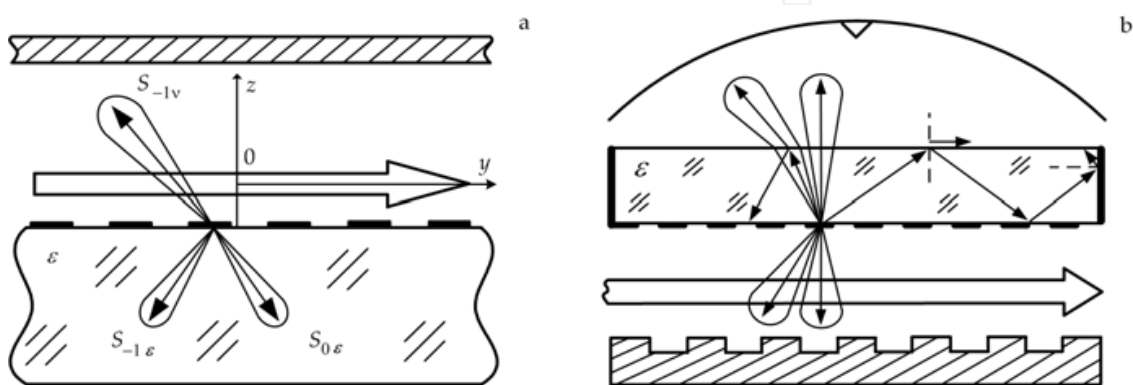

Fig. 6. Quasi-optical resonators based on metal-dielectric slabs

A more complicated case of the open resonator with a metal-dielectric structure is shown in Fig. 6b. The resonator consists of a spherical mirror, a plane mirror such as a reflecting diffraction grating, and a layered metal-dielectric structure between the two mirrors. Such an electromagnetic structure is often used in Cherenkov diffraction oscillators. Fig. 6b demonstrates possible modes of Cherenkov diffraction radiation excited by a source of electromagnetic energy distributed between the metal-dielectric grating and plane mirror.

The metal-dielectric slab (Fig. 6b) of the open resonator introduces qualitatively new electromagnetic properties in such a system. It is possible to attenuate the power in the open resonator, increase the amplitude of the oscillating wave and the value of Q-factor as well as to improve selectivity by choosing parameters of the metal-dielectric slab.

3. Coupled open waveguides employing periodic structures

This section describes the main properties of quasi-optical open waveguides with periodic metal-dielectric structures excited by distributed sources of electromagnetic energy such as electron beam or surface wave of a dielectric waveguide. Such structures are promising for the design of low-voltage amplifiers based on Smith-Purcell effect [Weinstein and Solntsev, 1973; Smith and Parcell, 1953] and other microwave and millimeter wave electron devices [Joe et al., 1994, 1997].

3.1 Amplifiers based on Smith-Purcell effect
Fig. 7 shows the structure of the amplifier using a planar layered metal-dielectric stack and based on Smith-Purcell effect. The open waveguide of the considered system consists of the

periodic rectangular grating structure **1** with the period of 2*l*, width 2*d* and grating depth of *h*; the planar layered metal-dielectric structure **2** with the thickness $\Delta = H - s$ which is positioned in parallel to the grating at a distance *s*. A non-relativistic sheet electron beam **3** with the finite thickness (r-b) is propagating along the axis 0y at a distance *b* above the grating. The entire structure is considered to be infinite within the plane x0y.

The electromagnetic problem is solved using the method of partial domains. The field in each domain is determined from the Maxwell equations, equation for the electron beam propagation, and corresponding boundary conditions. In order to obtain the dispersion equation, we have to perform the following operations: determine the linear approximation of the equation for the variable component of the convectional current intensity and the field in the beam, and transform it into a homogeneous form; determine the electromagnetic field in the interaction region in hot (with electron beam) and cold (without electron beam) regime.
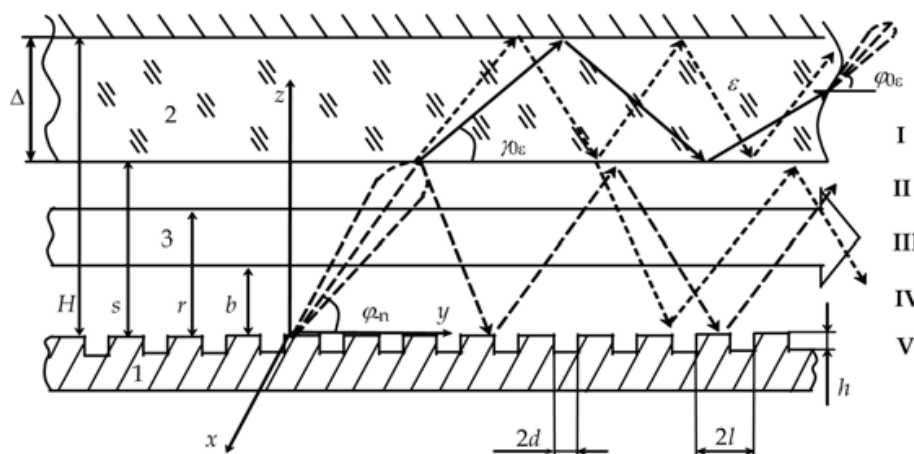

Fig. 7. The amplifier with the metal-dielectric layer based on the Smith-Purcell effect: 1 - periodic metal structure, 2 - planar layered metal-dielectric structure, 3 - electron beam

To this end, the electric field E, the beam velocity v_0, and the charge density ρ_0 are expressed as a sum of constant and small harmonically time-dependent variable quantities [Shmatko, 2008]. The charge density constant ρ_0 of the beam is considered to be compensated by external sources. The solution of the problem in such a way leads to the following dispersion:

$$1 + \frac{k}{ld}\tan kh \sum_{n=-\infty}^{\infty} \frac{\sin^2 \alpha_n d}{\alpha_n^2}\left[\frac{\Gamma_n\left(\cos\left(\xi_n\Gamma_n(b-r)\right) - \sin\left(\xi_n\Gamma_n(b-r)\right)\Pi\right)}{\Pi + \sin\left(\xi_n\Gamma_n(b-r)\right)}\right] = 0 , \qquad (3)$$

where $\Pi = \dfrac{\Gamma_n\cos\left(\xi_n(r-s)\right)\dfrac{\sigma_n}{\varepsilon\xi_n}\tan\left(\varsigma_n(s-H)\right) + \sin\left(\xi_n(r-s)\right)}{\cos\left(\xi_n(r-s)\right) - \dfrac{\sigma_n}{\varepsilon\xi_n}\tan\left(\varsigma_n(s-H)\right)\sin\left(\xi_n(r-s)\right)}$; $k = \dfrac{\omega}{c}$ - is the wave number;

ω - is the frequency; c - is the speed of light; ε - is the relative permittivity of the dielectric layer; $\alpha_n = \alpha_0 + \dfrac{\pi n}{l}$ - is the propagation constant of the electromagnetic wave propagating

along the axis 0y; $n = 0, \pm 1, \pm 2$ - is the spatial harmonic number; $\xi_n = \sqrt{\kappa^2 - \alpha_n^2}$, $\sigma_n = \sqrt{\varepsilon\kappa^2 - \alpha_n^2}$ - are the transverse wave numbers; $\kappa = \dfrac{kl}{\pi}$; $\Gamma_n = \sqrt{1 - \dfrac{\omega_p^2}{\left(\omega - v_0\alpha_n\right)^2 - \omega_p^2}}$; $\omega_p = \sqrt{\dfrac{e\rho_0}{m_e\varepsilon_0}}$ - is the plasma frequency of the electron

beam (e and m_e - are the charge and the mass of the electron, ε_0 - is the electric constant).

The following analysis of equation (3) concerns defining the propagation constant α_n, which is generally a complex number. The imaginary part $-i\alpha_n$ is responsible for the solutions increasing along the axis 0y and specifies the electromagnetic wave amplification in the system. The analysis of the given dispersion equation would be difficult without simplifications. If we separate this equation in three terms, which correspond to zeroth order harmonic, first harmonic, and the sum of the rest harmonics, and then use an approximation of the maximum interaction between the electron beam the fields of the slow wave structures (b = 0, s = r), it is possible to reformulate (3) into the following:

$$\frac{\cot\left(\pi\kappa\delta\right)}{\kappa\theta} = \frac{1}{\sqrt{\left(\mu+1\right)^2 - \kappa^2}}\left(\frac{\Gamma_1\left(1+\Gamma_1 FM\right)}{\Gamma_1 F + M} - 1\right) - \left(2\ln\left(\sin\left(\frac{\pi\theta}{2}\right)\right) + \frac{\varepsilon\cot\left(\pi\chi\sqrt{\varepsilon\kappa^2 - \mu^2}\right)}{\sqrt{\varepsilon\kappa^2 - \mu^2}}\right), (4)$$

where

$$\Gamma_1 = \sqrt{1 - \frac{g^2\kappa^2}{\left[\kappa - \beta\left(\mu+1\right)\right]^2 - g^2\kappa^2}}; \ M = \tanh\left(\pi\zeta\Gamma_1\sqrt{\left(\mu+1\right)^2 - \kappa^2}\right); \ F = \frac{\sqrt{\varepsilon\kappa^2 - \left(\mu+1\right)^2}}{\varepsilon\sqrt{\kappa^2 - \left(\mu+1\right)^2}}; \ g = \frac{\omega_p}{\omega}$$

is the spatial charge parameter, in practice $g \leq 0,01$; $\beta = \dfrac{v_0}{c}$ - is the relative electron beam

velocity, $\mu = \kappa\hat{\alpha}_n - 1$; $\hat{\alpha}_n = \dfrac{\alpha_n}{k}$ - is the unitless propagation constant;

$\gamma = \dfrac{h}{l}$, $\zeta = \dfrac{b}{l}$, $\theta = \dfrac{d}{l}$, $\chi = \dfrac{H}{l}$ - are the unitless geometrical parameters of the system.

The solution to the dispersion equation is found by using Newton iterative method for the range of electron velocities $\beta = 0,05 \div 0,2$ and various values of the electromagnetic parameters of the system κ, χ, ζ and $\varepsilon = 1 \div 210$. The lower ε limit corresponds to the case where there is no dielectric between the grating and the metal mirror; the upper limit corresponds to the case when it is possible to excite Cherenkov radiation at non-relativistic electron beam velocities ($\beta \approx 0,07$).

The numerical analysis of the dispersion equation for an open waveguide with no dielectric layer shows that there are two direct waves and two waves traveling in the backward direction exist in the system without the presence of an electron beam. They have different wave numbers and corresponding phase velocities. In addition to the previously described electromagnetic waves in the open waveguide, there are also two electron beam waves: a fast space-charge wave and a slow space-charge wave. All four electromagnetic waves in the system while synchronized with the electron beam spatial waves have regions with a

positive amplitude growth that allows for signal amplification and realization of the following regimes varying parameter β: surface wave mode with the maximum amplitude exists when synchronized with the slow space-charge wave; the volume waves of the diffraction radiation at the angle less than $\pi/2$ with respect to the grating plane which transfer power from the beam to the field by means of the slow and fast space-charge waves. It must be noted that the regime employing fast space-charge wave is observed starting from the relative beam thickness $\zeta = 0,6$, and the regime employing slow space-charge wave is observed starting from $\zeta = 0,02$. Depending on the excitation region the maximum amplitude of the amplified signal is observed at $\zeta = 0,4 \div 0,6$ that corresponds to the electron beam thickness $r \approx 0,1$ mm, which is typical for the microwave tubes. The further increase in r has no influence on the amplitude of the amplified signal but results in generation of a discrete set of radiated electromagnetic waves the number of which depends on thickness of the electron beam and the frequency. This effect can be physically explained by the dispersion properties of the electron beam and partial reflection of the electromagnetic waves from its boundaries (equivalent of the low reflection coefficient resonator).

Introducing a dielectric layer with small values $\varepsilon \approx 3$ will result in changing the phase velocities of the electromagnetic waves in the open resonator and synchronization with the electron beam. This also leads to the generation of additional waves with the parameters close to those for the case with $\varepsilon = 1$. Transverse wave numbers σ_n, ξ_n (3) determine the wave modes classification in the open waveguide: volume waves propagating between the periodic structure and the metal plane; the volume waves in the dielectric layer; the surface waves above the periodic structure.

The increase in permittivity ε of the dielectric layer leads to accumulation of power from volume waves that is caused by the improvement of its resonance properties due to reflection from the boundaries of the dielectric. Fig. 8 represents graphically the solution of the dispersion equation with regard to the real (Re μ) and imaginary (Im μ) parts of the gain factor versus the parameter β for $\varepsilon = 50, \kappa = 0,083, \chi = 10$. The presented curves allow to analyze the propagation properties for fourteen wave modes in the open waveguide, two of which, 7 and 8, are the fast and slow space-charge waves of the electron beam respectively. The waves from 1 to 6 are propagating in the same direction as the electron beam propagation, while the waves 9 and 10 are propagating in the opposite direction. The parameters of the mentioned waves satisfy the condition for their propagation in the dielectric layer. Consequently, the increase of the number of wave modes in the open waveguide results in distribution of the energy between them and leads to a decrease of the amplitude growth factors for some waves as compared to the case when $\varepsilon = 1$.

Parameter χ (the distance between the mirrors of the open waveguide normalized to the grating period) has a significant influence on the propagation properties of the modes and defines the field distribution between the mirrors of the open waveguide. Fig. 9 graphically represents the solution of the transcendent equation (4) with regard to the real and imaginary parts of the gain factor versus β for different values of the parameter χ and the direct volume wave of the periodic structure ($\varepsilon = 1$). The presented data illustrates that changing the distance from $\chi = 8$ to $\chi = 14$ leads to a considerable decrease in the amplitude of the signal. The maximum amplitude of the signal is observed at the radiation

along the normal direction ($\chi = 8$, $\mu \approx 0$) while the minimum is observed in a tangential direction ($\chi \approx 14$, $\mu \approx 0{,}073$). However, it is not possible to ensure the excitation of the traveling wave mode along the axis of the open waveguide for radiation in the normal direction. In practice, this would result in a feedback and instability. This operation mode is similar to the operation of the microwave tubes such as orotron and diffraction radiation oscillator [Shestopalov, 1991].

It should also be noted that increasing the distance between the mirrors results in increase of a number of surface waves and decrease of the gain factor for the volume waves. In the extreme case when the values $\chi \rightarrow \infty$, the volume waves transfer into surface waves and the system is similar to the traditional devices such as the backward-wave oscillator and the traveling-wave tube.
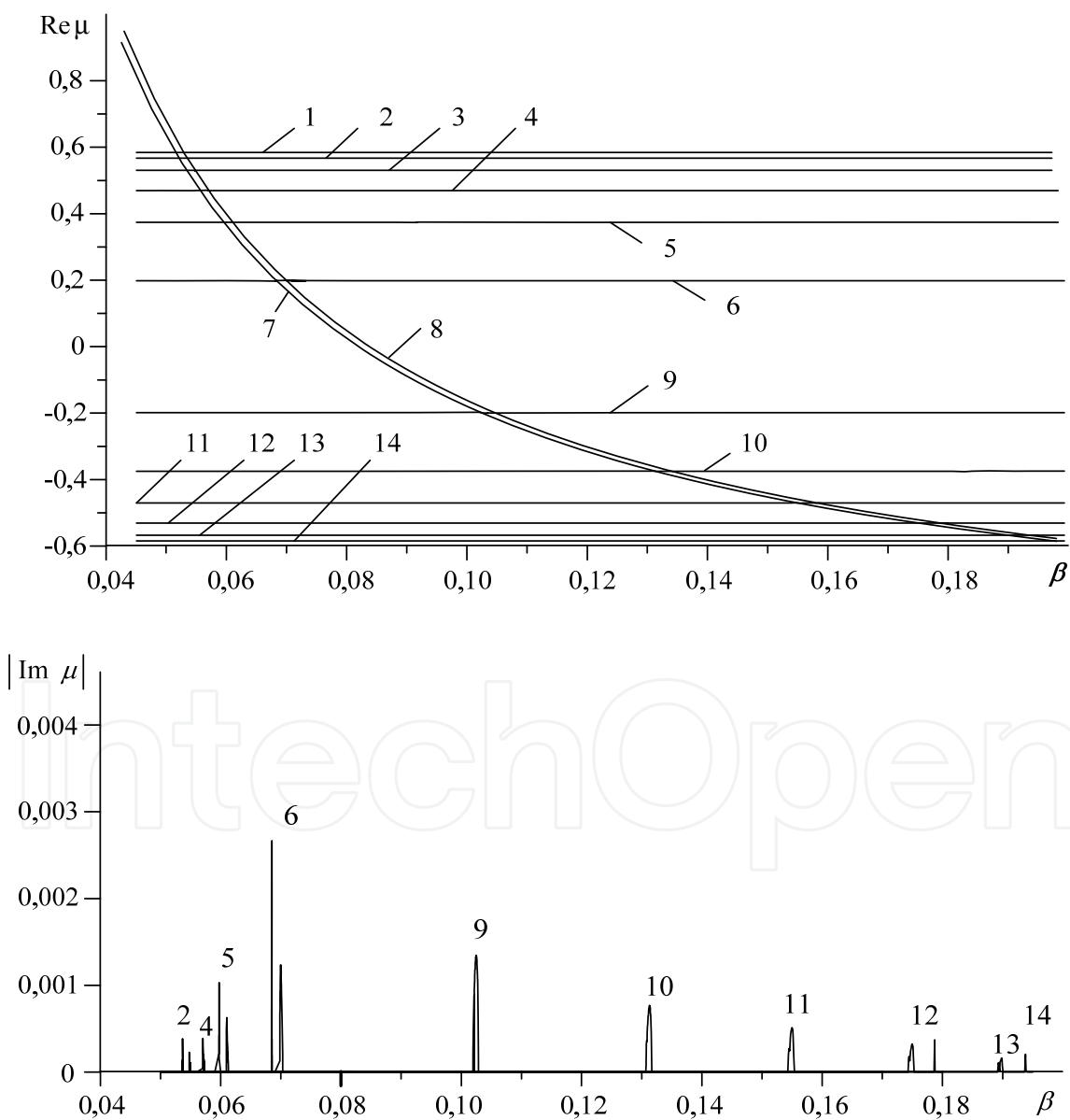
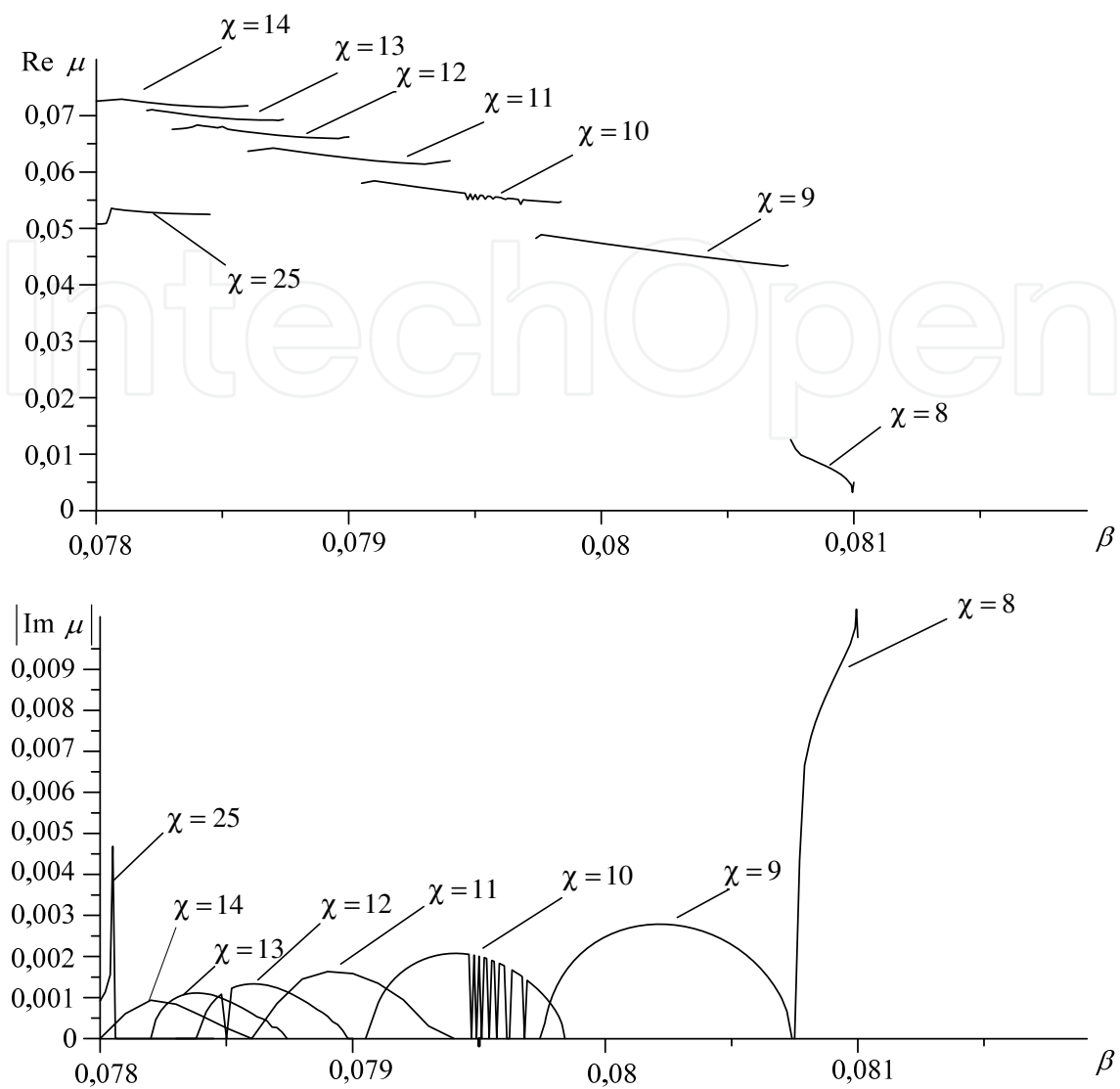Fig. 8. Solutions of the dispersion equation (4) for $\varepsilon = 50$

Fig. 9. Influence of the parameter χ on the solutions of the dispersion equation (4) for $\varepsilon = 1$

3.2 Experimental modeling of coupled open waveguides

The experimental modeling is one of the most efficient methods for solving problems of diffraction electronics. The radiation of the electron beam is simulated by a surface wave in the planar dielectric waveguide placed above the diffraction grating. The modeling techniques have been sufficiently developed and summarized in the literature [Shestopalov, 1976, 1985, 1991]. Nevertheless, each structure has its own specific features which have to be taken into account while developing and realizing the experimental setup.

There are three components in the previously described electromagnetic system which can be considered separately during the experimental modeling of the wave processes in amplifiers based on Smith-Purcell effect. They determine the general electromagnetic properties of the open waveguide. These components are the dielectric waveguide which feeds the surface wave into the system; diffraction grating which transforms the surface wave from the dielectric waveguide into the volume wave; the planar layered metal-dielectric structure which serves for both a transformation of the surface wave into the volume wave for the dielectric layer and reflection of the radiation arriving from the

diffraction grating - dielectric waveguide interface. Compared to the system without the metal-dielectric layer, the wave processes in the open waveguide with the metal-dielectric stack are more complicated in comparison to the systems without such a stack due to the presence and superposition of different waves such as the volume wave incident to the layered metal-dielectric structure from the diffraction-grating-dielectric-waveguide interface and the waves propagating in the dielectric.

The parameters of the diffraction-grating-dielectric-waveguide system are chosen to satisfy the condition of the volume wave existence in the open waveguide [Shestopalov, 1991]:

$$\varphi_{-1} = \arccos\left(1/\beta_w - n/k\right),$$ (5)

where φ_{-1} - is the radiation angle, $\beta_w = v_w/c$ - is the relative velocity of the wave in the waveguide, v_w - is the phase velocity, $k = l/\lambda$ - is the wave number, λ - is the wave length.

The period of the diffraction grating has been chosen such that the main lobe of the radiation pattern ($n = -1$) is at an angle $\varphi = 70°$ for the wavelength of 9 mm and the parameter $\beta_w \approx 0,9$ which corresponds to the material of the dielectric waveguide implemented in the experiment (polystyrene waveguide with a cross-section $7,2 \times 3,4\ mm^2$). The depth of the grating slots was chosen to minimize the influence of their resonance properties on the radiation characteristics. The waveguide length L is 150 mm, that satisfies the requirement $L/\lambda \geq 10$. This ensured the excitation and propagation of electromagnetic wave along the open waveguide axis.

The distance between the dielectric waveguide and the surface of the diffraction grating, a, is a very important parameter for the optimization of the system. The diffraction of the surface waves on the diffraction grating is nontrivial in this case because the value a is chosen to be smaller than the wavelength. However, a strong coupling between the waveguide and the diffraction grating effects the field distribution in the waveguide and, consequently, the propagation constant β_w. The strong coupling results in interference between the wave propagating along the waveguide and the wave being scattered by the diffraction grating. Such an interference might result in additional propagation modes in the waveguide and, consequently, in the parasitic spatial harmonics [Shestopalov, 1991].

The behavior of the planar metal-dielectric structure of the open waveguide is similar to the behavior of the shielded planar dielectric waveguide. In order to analyze the physical phenomena of the electromagnetic wave excitation in the layered metal-dielectric structure, the electromagnetic field can be represented as a composition of plane electromagnetic waves. Based on this, the metal-dielectric structure can support two types of waves: the one excited by the diffraction grating-dielectric waveguide interface (these waves not necessarily undergo total internal reflection in the dielectric for certain angles φ_{-n}); the second type of waves is excited by a guided surface electromagnetic wave in the dielectric waveguide and is totally reflected from the boundaries of the layered metal-dielectric structure (the wave satisfies the following condition $\cos\gamma_{0\varepsilon} = cv_w/\sqrt{\varepsilon}$)(see Fig. 7). The second wave allows to model Cherenkov radiation. However, this concept of wave decomposition does not consider the multimode nature of the metal-dielectric wave-guiding structure. The modes exist due to the finite layer thickness Δ comparable to the wavelength. The metal layer on the side wall of the dielectric does not prevent the wave propagation but results in increase

of the effective thickness of the layer and number of the higher order modes in the metal-dielectric structure.

The experiments were performed in the frequency range from 30 GHz to 37 GHz within the interval $\Delta \approx \lambda - 4\lambda$ and using a dielectric with permittivity $\varepsilon = 2$.

Fig. 10 shows of the normalized radiation pattern in the open waveguide at the center frequency $f = 33,4\,GHz$. The diagrams in Fig. 10a depicts the radiation from the end of the metal-dielectric structure in the mode of Cherenkov radiation for the phase velocities satisfying the condition $\varepsilon\beta_w^2 > 1$ for guiding electromagnetic wave on the homogeneous surface of the dielectric. Propagation of the most portion of power in the surrounding environment is typical for the dielectric layer with the thickness less than the wavelength (Figure 10a - curve 1). This holds when the single-mode condition satisfies the condition of synchronization between the phase velocities of waves in dielectric and wave in the surrounding environment. The dielectric layer is actually operates as an antenna, which radiates the power in the direction close to the axis y. The observed asymmetry in the patterns is caused by the technical difficulties to measure the radiation at angles $\varphi_{0\varepsilon} \approx 0 - 10°$. The side lobes are caused by the mismatch with the open area, multiple reflections from the measurement setup, and by a power leakage from the dielectric-waveguide-to-metallic-waveguide transitions. The observed peaks in the radiation pattern are due to the strong coupling between the dielectric waveguide and the dielectric layer at the center and critical frequencies.
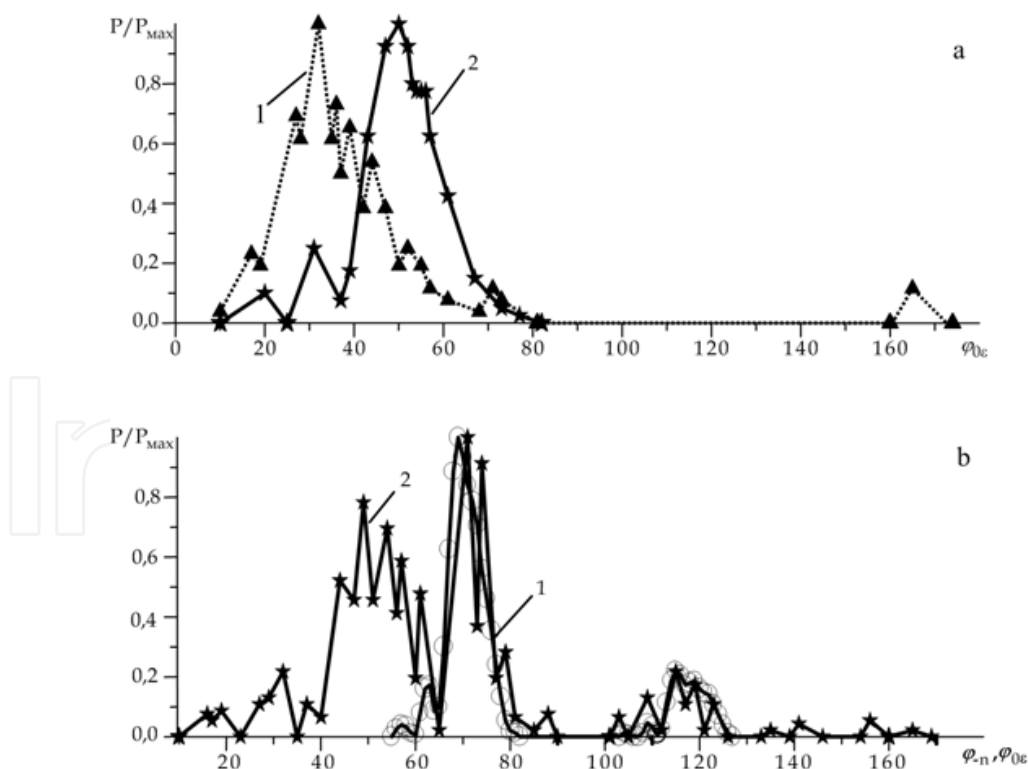

Fig. 10. Radiation patterns of the open waveguide components: a - dielectric layer - dielectric waveguide ($\Delta \approx \lambda$ - curve 1, $\Delta \approx 4\lambda$ - curve 2); b - diffraction-grating-dielectric-waveguide (curve 1), diffraction-grating-dielectric-waveguide-dielectric-layer system (curve 2)

For dielectric layers with $\Delta > \lambda$, the wave is totally reflected from the boundaries and a significant portion of the power is concentrated in the dielectric. The direction of radiation from the end changes to a higher angle (Fig. 10a - graph 2) and approach the calculated values determined from the geometrical optics ($\varphi_{0\varepsilon} \approx 62°$ at $\gamma_{0\varepsilon} \approx 39°$, Fig. 7).

Fig. 10b (curve 1) demonstrates the patterns of the diffraction-grating-dielectric-waveguide radiating system. It is clear from the presented data that the main radiation maximum is in agreement with the calculated value of $\varphi_{-n} = 70°$. At such an angle, the beam for $\varepsilon = 2$, which incidents side wall of the dielectric layer, is slightly refracted and leaves the dielectric from the opposite side at an angle, which is approximately equal to the angle of radiation. This fact is illustrated in Figure 10b for the diffraction-grating-dielectric-waveguide-dielectric-layer system for $\Delta \approx 4\lambda$ (graph 2).

Covering the dielectric layer with a metal (Fig. 7) results in the fact that the radiation arriving from the diffraction-grating-dielectric-waveguide system will be reflected and fed into the open waveguide volume exciting the wave along its axis. Correspondingly, there are two volume waves propagating in the system: the wave in the layered metal-dielectric structure and the wave in the volume of the open waveguide. These waves are coupled to each other by means of the surface wave of the common radiation source - the dielectric waveguide. The existence of the forward and backward coupled waves in the open waveguide might result in parasitic resonances during the modeling. The wave numbers are complex if there is a coupling between the direct and the backward waves. This indicates the excitation of complex decaying waves. The waves are synchronized and the power of the forward wave is pumped into the backward wave and vice versa. Such a power exchange is performed along the significant propagation distance if the coupling is weak. The propagation becomes impossible and the transmission line turns into a sort of a resonator for certain frequencies. In such a system the waveguide characteristics such as the standing wave ratio (SWR) and the transmission coefficient ($K_{tr} = P_{output}/P_{input}$, where P_{output} and P_{input} are the power values at the dielectric waveguide output and input respectively) become fundamental. The waveguide characteristics of the dielectric-waveguide-dielectric-layer system (curve 1), dielectric-waveguide-diffraction-grating-dielectric-layer system (curve 2) and the open waveguide system in general (curve 3) are represented in Fig. 11 for $\Delta \approx \lambda$. The presented data indicates that the SWR of the open waveguide elements and the system in general are within the interval $1,05 \div 1,4$. These reflections are due to the out of band mismatch of the dielectric-waveguide-metallic-waveguide transitions. The achieved SWR is considerably different from SWR for the open waveguide with no dielectric layer which is approximately 2,0 (curve 4) due to the resonance nature of the system. Substantial changes in the behavior of the K_{tr} versus frequency are also observed. Curves 1 and 2 indicate an efficient transformation of surface waves into the volume waves, while graph 3 indicates the presence of the coupled waves in the system and it is substantially different from the behavior of K_{tr} for the open waveguide with no layered metal-dielectric structure in it (curve 4). It can be assumed that for $\Delta \approx \lambda$ a large amount of power escapes from the dielectric and propagates in the open waveguide. The observed maxima and minima of the spectrum of K_{tr} can be explained by the fact that the waves propagating in the open waveguide are combined in- and out of phase.

The increase in the thickness of the dielectric layer results in the fact that the most amount of power is concentrated in the dielectric which leads to decrease in coupling between the layered metal-dielectric structure and the dielectric waveguide, and, in general, increase in K_{tr} for the open waveguide components (Fig. 12, curves 1 and 2) at $\Delta \approx 4\lambda$.

At the same time, the behavior of the transmission coefficient in the considered frequency band indicates the decrease in the coupling between the waves propagating in the open waveguide (Fig. 12, curve 3).

The analysis described above for the characteristics of the open waveguide and its components indicates that it is possible to control the electromagnetic processes in the system by varying the thickness of the dielectric layer: adjust the coupling between the radiation of the dielectric waveguide and the waves propagating in the open waveguide. The increase in coupling is useful for enhancing the efficiency of the interaction between the electron beam and the open waveguide fields in the amplifier applications. The decrease in the coupling is interesting for realization of power decoupling from the open waveguide through the dielectric layer.

Fig. 11. Waveguide characteristics of the open waveguide components at $\Delta \approx \lambda$ - dielectric-layer–diffraction-grating system; 2 - diffraction-grating-dielectric-waveguide-dielectric-layer system; 3 - open waveguide with the dielectric layer; 4 - open waveguide without the dielectric layer
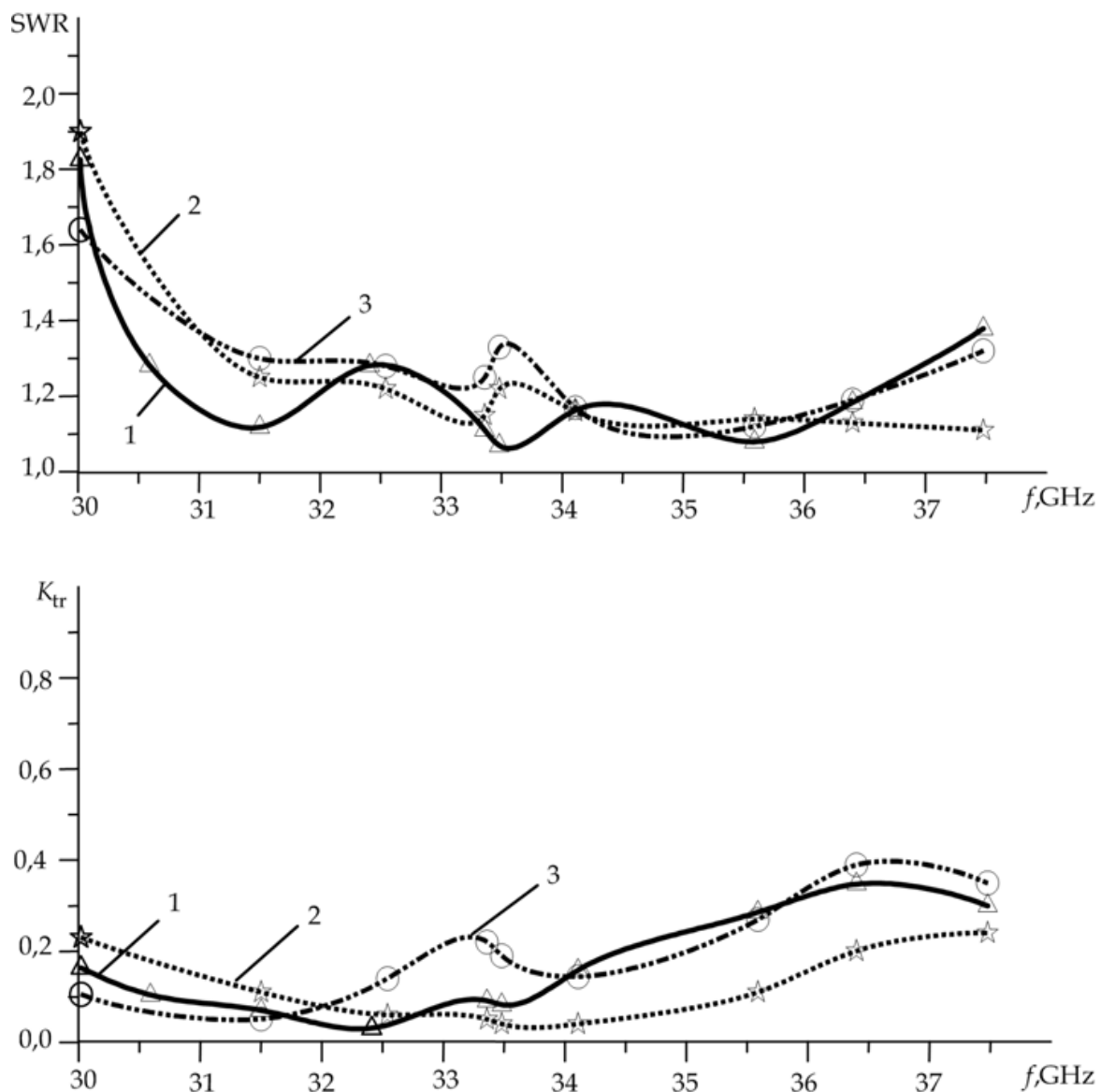
Fig. 12. Characteristics of the open waveguide components at $\Delta \approx 4\lambda$: 1 - dielectric-layer–dielectric-waveguide system; 2 - diffraction-grating-dielectric waveguide-dielectric-layer system; 3 - open wavegude with the dielectric layer

4. The implementation of coupled quasi-optical systems in vacuum electron devices

A two-stage diffraction radiation oscillator has been realized using the structure shown in Fig. 2a in the frequency range $f = 43 \div 98\,GHz$. The system consists of two short-focus spherical mirrors [Shestopalov, 1991] and the common cylindrical mirror with a diffraction grating along its longitudinal axis. The electron beam generated by the electron gun and focused by the static magnetic field propagates above the diffraction grating exciting electromagnetic oscillations in the coupled open resonators. In case of weak coupling between the open resonators, the device operates as a multifrequency oscillator at specific frequencies. In case of optimal coupling, the device operates as a broadband diffraction

radiation oscillator with coupled resonators. The operating frequency band in this case is more than 1,5 times wider compared to the single resonator diffraction radiation oscillator.

The device operates as an amplifier if the microwave signal is applied to the input of the first (with respect to the gun) resonator and the beam current J is less than the starting current J_n. These regimes have been tested in the millimeter wave range ($f = 43 \div 98\,GHz$). Figure 13 shows the data when the device operates as an oscillator in case of optimal coupling between the open resonators. The power of such a diffraction radiation oscillator at $f_0 = 84\,GHz$ was measured to be 0,4 W with the beam current $J = 1,5J_n\,(J_n \approx 30\,mA)$. The range of electron frequency tuning at these conditions was 1,5 times wider than in the case of a single-resonator oscillator, which is comparable with the results obtained by the previously described modeling (Fig. 4). A similar behavior has been also observed in the regime of amplification at $J \approx 0,8 \div 0,9J_n$, which confirms the possibility to build a regenerative amplifier based on coupled open resonators with a broader transmission band than just using a single-resonator amplifier [Shestopalov, 1991].
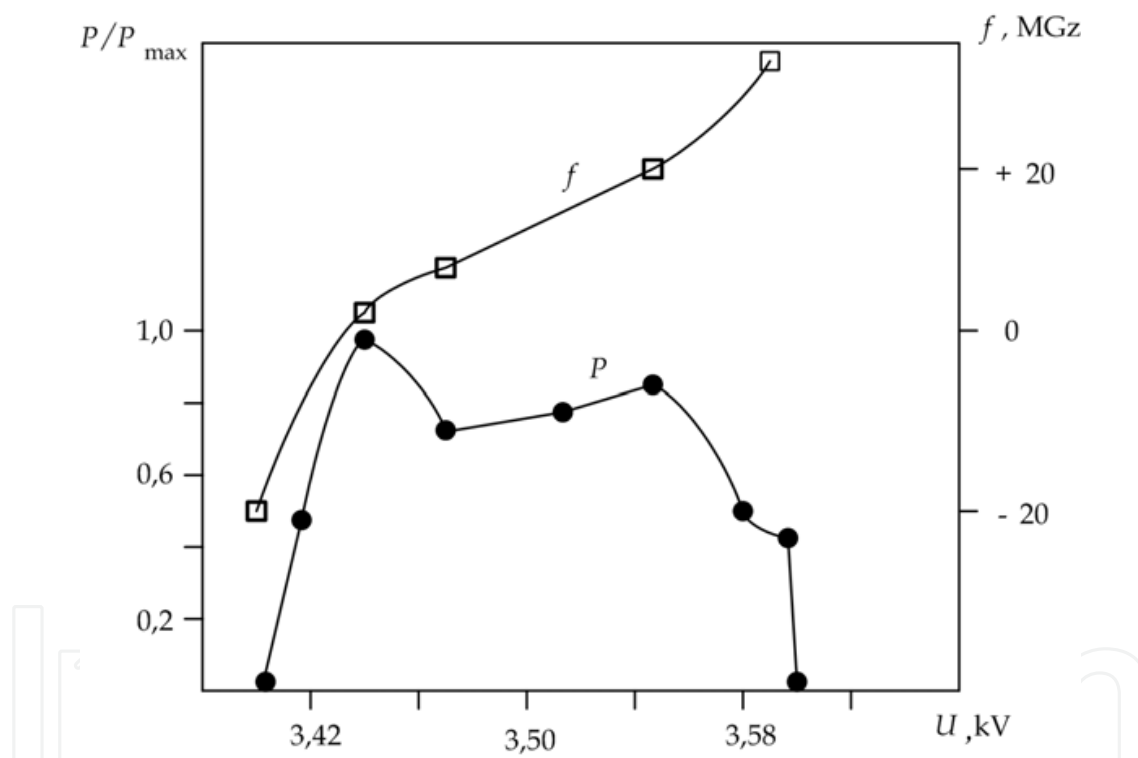

Fig. 13. The bandwidth and a tuning range of the diffraction radiation oscillator based on two coupled resonators

Figure 14 presents the diagrams of a vacuum electron devices with open resonators connected in series with respect to the axis of the electron beam. An orotron shown in Fig. 14a consists of two coupled open resonators **1**. Each of these resonators consists of two mirrors **2** and **3**. Energy is coupled out through a waveguide in mirror **2**. Mirror **3** has a parabolic cylinder shape. Metal-strip diffraction gratings **4** located in the center of the adjacent parabolic mirrors **3** are made of metal bars. The electron gun **5** generates a focused electron beam **6** and is placed between the parabolic mirrors **3**. A collector **7** is positioned at the end of the interaction region.

The operation of the orotron can be described in the following way: the electron gun generates a focused electron beam which than experiences a bunching within the small interaction length due to the spatial charge in the interaction zone formed by the open resonators and gratings. The diffraction radiation is produced in the open resonators as electrons propagate through the gap between the diffraction gratings. The electrons are than striking a collector at the other end of the interaction region. The orotron operates as an oscillator if the electron beam current is much higher than the starting current. The orotron operates as an amplifier if the condition of self-excitation is not satisfied and a signal from an external microwave source is fed to the input of one of the resonators. It should also be noted that the orotron may function as a frequency multiplier if using two coupled open resonators. This device is a low-power oscillator. The increase of the electron beam current density is limited due to overheating of the strip diffraction grating.
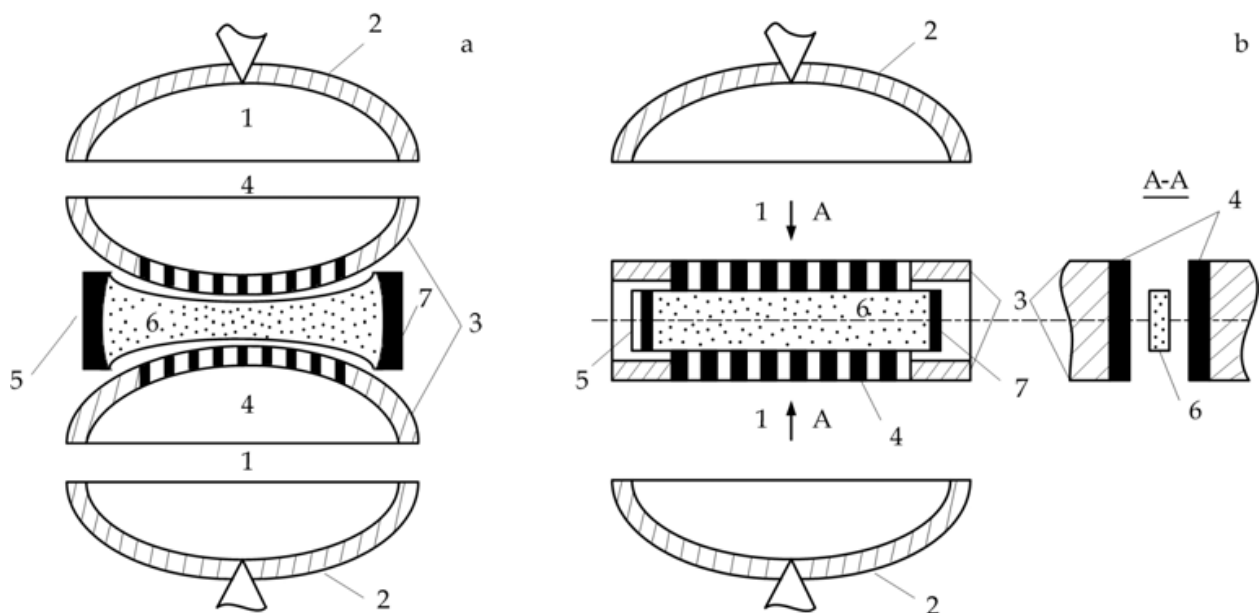

Fig. 14. Vacuum electron devices based on parallel connection of open resonators: a - an orotron with coupling through the strip diffraction gratings and b - diffraction radiation oscillator with coupling through the reflective diffraction gratings

A higher power level can be achieved in diffraction radiation oscillators based on coupled open resonators schematically shown in Fig. 14b. The design and the principle of operation of such a device are similar to the design and the principle of operation of the previously described orotron. The coupling of resonators **1** is achieved through the slots in the identical reflective diffraction gratings **4** placed in the center of the adjacent mirrors **3** and perpendicularly oriented with regard to the planes of these mirrors. The electron beam is focused with a magnetic field. The use of bulky gratings attached to the mirrors simplifies the temperature dissipation and, consequently, allows for higher electron beam currents. Furthermore, one of the resonators in such a system may be realized with an option for mechanical tuning where a moving short-circuit plunger located on the opposite side of the coupling slot. Figure 15 shows the oscillation bandwidth and frequency tuning characteristic for different distances h of the plunger for the case when the open resonator is centered at $f_0 = 36\ GHz$.
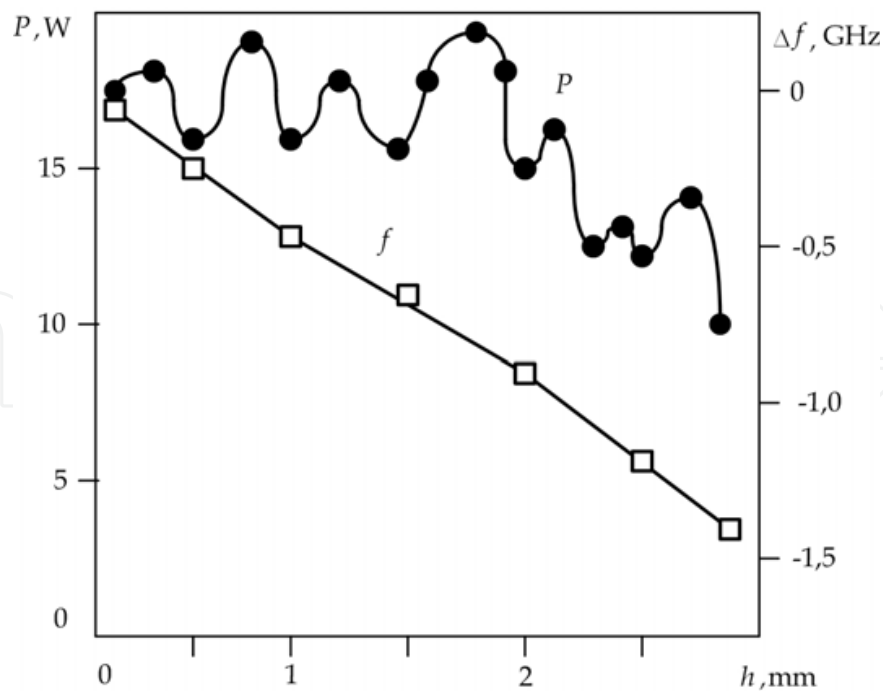
Fig. 15. The output power and the frequency tuning range of the diffraction radiation oscillator with a tunable resonator coupled to the open resonator

The presented data shows that, one can smoothly tune the oscillation frequency within a sufficiently broad frequency range by mechanically tuning the volume resonator with a fixed value of H for the mirrors in the open resonator. The variation of the output power in the considered frequency band does not exceed 3 dB. This characteristic of the considered device indicates the possibility for improving the vibration stability of the system in comparison to the vibration stability of systems with mechanical tuning of mirrors. The grating-coupled open resonators could also be used to build reflection type diffraction radiation oscillators [Shestopalov, 1991]. In this case, the collector should be replaced by an electron reflector, producing a backward electron beam. Such devices exhibit low starting currents and able to operate in the regime of stochastic oscillations [Korneenkov et al., 1982]. The wide functionality of open resonators with layered metal-dielectric structures allowed to build several types of diffraction based devices with complex resonant structures such as Cherenkov diffraction oscillator and Cherenkov backward-wave tube. Fig. 16 shows the example of Cherenkov backward-wave tube and Cherenkov diffraction oscillator.

The electron beam **1** of the backward-wave tube is generated by the electron gun **2**. The beam propagates through the channel **3** formed by the adjacent surfaces of the resonator **4** to the slow-wave structure **5**. The electron beam interacts with the field of the slow-wave structure **5** resulting in modulation of charge density. Simultaneously, Cherenkov radiation occurs when the electrons velocity exceed the phase velocity of the electromagnetic wave in the dielectric. The radiation is directed into the dielectric. The resonator **4** has a field distribution allowing a feedback (solid lines with arrows). Oscillations occur in the resonator effectively extracting power from the modulated electron beam via the strip grating **6** when the frequency is synchronized with the eigen frequency of the resonator. The power is coupled from the resonator **4** via the waveguide **7** with $\varepsilon_1 > \varepsilon$. The synchronization between the electron beam and the wave in the dielectric is achieved by choosing the proper value for ε and adjusting the accelerating voltage for the electron beam.
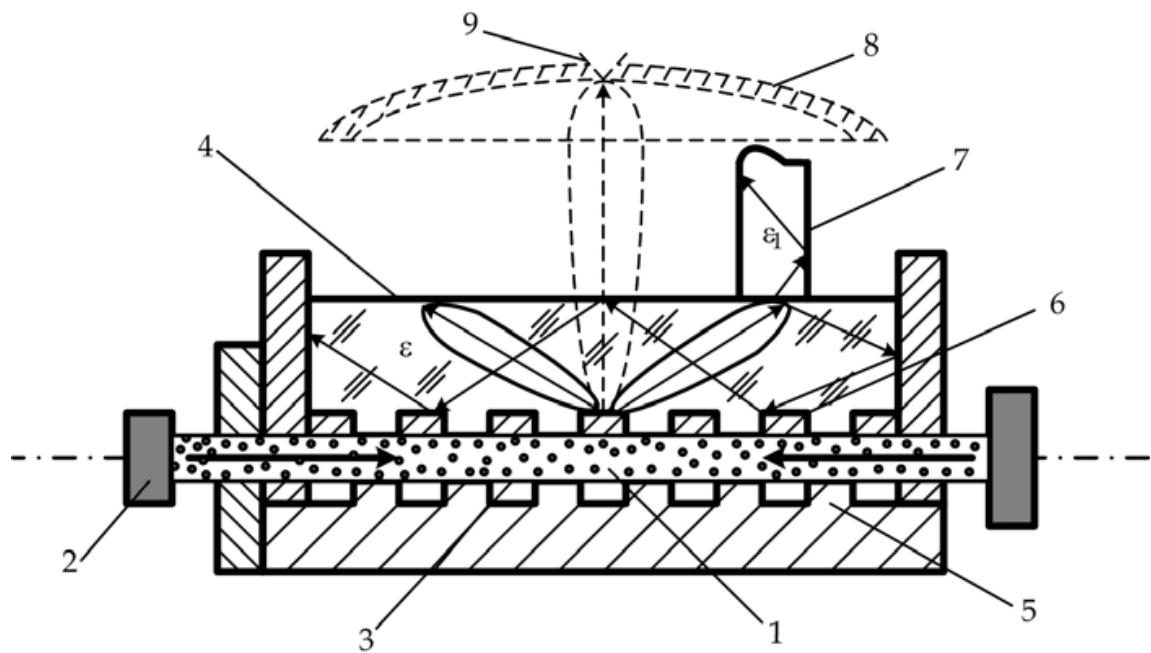
Fig. 16. Realization of Cherenkov backward-wave tube and Cherenkov diffraction oscillator

The similar electron optics is used for excitation of Cherenkov diffraction radiation. The slow-wave structure (diffraction grating) **5** is positioned in the central part of the fixed mirror. The moving mirror **8** with a coupling slot **9** is used for coupling the power out of the device. In contrast to the backward-wave oscillator, the geometrical parameters of the gratings **5**, **6** are optimized for efficient excitation of radiation in the normal direction with respect to the axis of the electron gun **2** (dotted oscillation pattern in Fig. 16) and for maximum power density of Cherenkov radiation within the dielectric resonator **4**.

Recently, significant attention is drawn to amplifiers based on Smith-Purcell effect, which has been described in section 3. An amplifier employing sheet electron beam is shown in Figure 17.
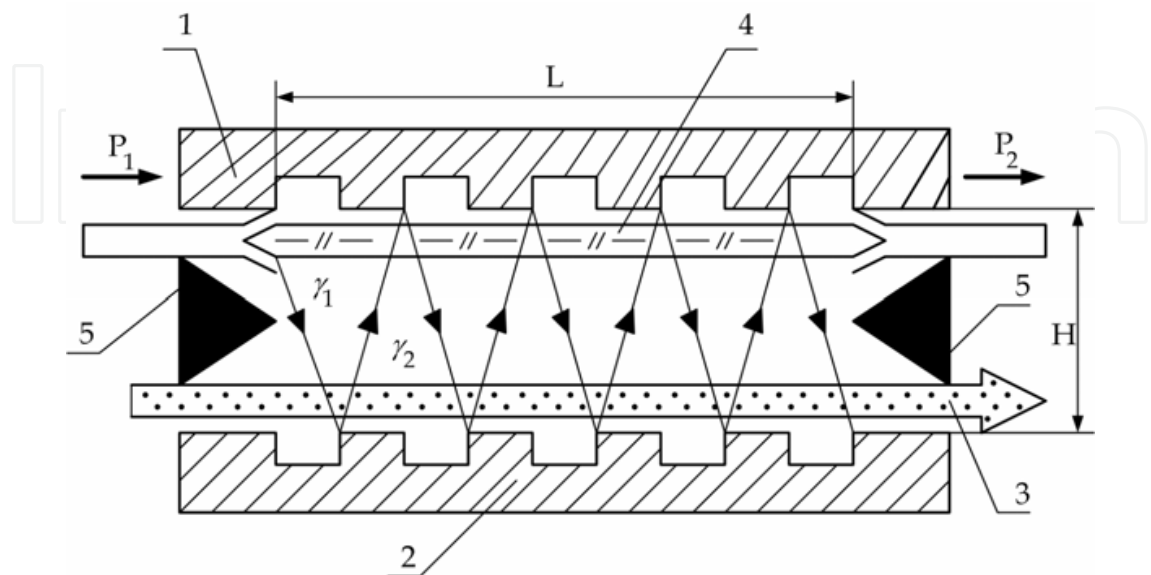

Fig. 17. Travelling wave tube based on the Smith-Purcell effect

The open waveguide with length L is formed by the surfaces of parallel passive **1** and active **2** mirrors realized as reflecting diffraction gratings with the periods l_1 and l_2 and a distance H between them. The sheet electron beam **3** propagates above the surface of the active mirror **2**. The dielectric waveguide **4** is placed close to the surface of the passive mirror **1**, and the matched absorption loads **5** are positioned at the ends of the waveguide. The periods l_1 and l_2 of the diffraction gratings comply with the relations that follow from the conditions of the in-phase mode of radiation (shown with arrows) from the active and the passive mirrors of the open waveguide:

$$l_1 = \frac{\lambda}{1 + \tilde{\varepsilon}_w \left(\sqrt{\varepsilon} - 1 \right) - \cos \gamma_2}; l_2 = \frac{\lambda}{5 / \sqrt{KU_0} - \cos \gamma_2}; \tag{6}$$

$$arctg \frac{2H}{L} + \left(\frac{65\lambda}{L} \right)^{\circ} \leq \gamma_2 < 90°; L \geq 10\lambda \, ,$$

where $\tilde{\varepsilon}_w = \dfrac{c^2}{v_w^2}$ - is the effective permittivity of the waveguide; U_0 - is the accelerating voltage of the electron beam, V; K=505 1/V.

The range of angle γ_2 and the length L of the waveguide are chosen to minimize diffraction loss into the free space. A high-frequency signal of power P_1 with a wavelength λ is fed to the dielectric waveguide **4**. The transformation of the surface wave into the volume wave radiated in the direction of angle $\gamma_1 = \arccos(c/v_w + \lambda/l_1)$ occurs on the diffraction grating of the passive mirror **1**. The non-reflected portion of the volume wave excites the spectrum of the spatial harmonics having different phase velocities when the volume wave of the transformed input signal incidents the grating of the active mirror **2**. The electron beam velocity v_e synchronizes with one of the surface waves which results in bunching of electrons radiating at a frequency of input signal in the direction of angle $\gamma_2 = \arccos(c/v_e + \lambda/l_2)$. The reverse transformation of the volume wave into the surface wave, which is followed by a radiation into the open waveguide, occurs at the grating of the passive mirror. The signal P_2 is amplified in the case of the in-phase radiation from the mirrors. The periodic re-emission results in increase of amplitude of the volume wave propagated along the open waveguide and the amplitude of the surface wave propagating in the same direction along the dielectric waveguide which is used to couple the amplified signal P_2 out to the load. The matched loads **5** and the dielectric waveguide **4** decrease the probability of regeneration effects that might occur in the amplifier both due to the reflections from the open waveguide ends and due to the parasitic oscillations due to multiple reflections between the active and the passive mirrors in direction of angles γ_1 and γ_2 close to $\pi/2$.

The prototype of the suggested travelling wave tube has been realized in the V band. The open waveguide was formed by two cylinder-shaped mirrors (the passive mirror with the curve radius $R_{curv} = 20 \, mm$ and the active mirror with $R_{curv} = 110 \, mm$). The grating periods l_1 and l_2 were chosen according to (6) resulting in $\gamma_1 = \gamma_2$. High-frequency signal was fed into the amplifier from the resonance carcinotron in the frequency band $f = 68 \div 72 \, GHz$

using a quartz dielectric waveguide and a sheet beam with a cross-section $5 \times 0,2 \ mm^2$. The electron beam was propagating along the active mirror with accelerating voltages in the range $U_0 = 2200 \div 2500 \ V$. The system was built in the vacuum shell between the poles of the electromagnet that limited the open waveguide length to L=40 mm and allowed to ensure about a double transformation of the surface wave into the diffraction radiation. The achieved experimental results show that amplification of rather broadband signals (up to 2 GHz) along with increase in gain is possible if increase the beam current. At the same time, the limited length of the open waveguide did not allow a sufficient number of transformations of the surface waves into the volume waves, which limited the increase of the gain K.

A further improvement of the output parameters of the amplifier could be achieved by increasing the interaction region and the electron beam current. This could be achieved, for instance, by means of using axial-symmetric electromagnetic systems and a better electron focusing optics.
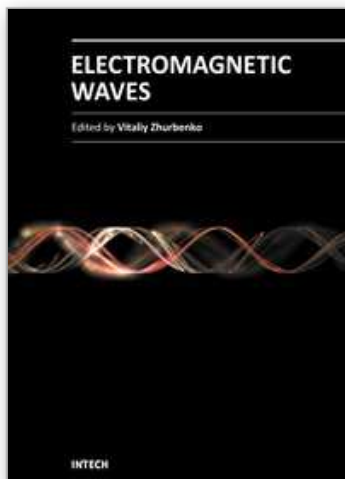
5. Conclusion

The chapter provides a summary of results on both the classical quasi-optical systems forming a basis for development of new modifications of oscillation systems of the microwave and millimeter-wave band devices and more advanced coupled electromagnetic systems with complex periodic structures such as coupled open resonators, open resonators and waveguides with layered metal-dielectric structures. It is demonstrated that the coupled open resonators exhibit wider frequency tuning range while preserving high values of Q-factor. Coupled systems such as open resonators and waveguides with layered metal-dielectric structures have qualitatively new properties: by varying the parameters of metal-dielectric structure one could achieve attenuation or amplification of the oscillations and their selection. New modifications of Cherenkov traveling wave tube such as Cherenkov diffraction oscillator and amplifier based on the Smith-Purcell effect are suggested and realized.

6. References

Balakirev, V.A., Karbushev, N.I., Ostrovsky, A.O., and Tkach, Yu.V. (1993). *Theory of Cherenkov amplifiers and oscillators based on relativistic interaction of oscillation bundles*, Naukova Dumka, Kyiv.

Belous, O.I., Fisun, A.I., and Sukhoruchko, O.N. (2003). Synthesis of basic components of a low-noise input circuit for millimeter wavelength. *Telecommunication and Radio Engineering*, Vol. 59, No 1-2, p.p. 111-118.

Bratman, V.L., Dumesl, B.S., and Fedotov, A.E. (2002). Broadband orotron operation at millimeter and sub-millimeter waves. *International Journal of Infrared and Millimeter Waves*, Vol. 23, No 11, p.p. 1595-1601.

Ginzburg, N.S., Zavolsky, N.A., and Zapevalov, V.Ye. (2000). Non-stationary processes in orotron with diffraction output of oscillation. *JTP*, Vol. 70, No 4, p.p. 99-104.

Joe, J., Scharer, J., Booske, J.H., and Mevey, B. (1994). Wave dispersion and growth analysis of low-voltage Cherenkov amplifiers. *Phys. Plasmas*, Vol. 1, No 1, p.p. 176-188.

Joe, J., Louis, L.J., Booske J.H., and Basten, M.A. (1997). Experimental and theoretical investigations of a rectangular grating structure for low-voltage traveling-wave tube amplifiers. *Phys. Plasmas*, Vol. 4, No 7, p.p. 2707-2715.

Korneenkov, V.K., Miroshnichenko, V.S., and Tsvyk A.I. (1982). About excitation of accidental oscillations in diffraction radiation oscillator-free electron laser. *Report. AN. USSR, Ser.A*, No 5, p.p. 59-61.

Marshall, E.M., Philips, P.M., and Walsh, J.E. (1998). Planar orotron experiments in millimeter wavelength band. *IEEE Transactions on Plasma Science*, Vol. 16, No 2, p.p. 199-205.

Milovanov, O.S., and Sobenin, N.P. (1980). *Microwave equipment*, Atomizdat, Moscow.

Rusin, F.S., Bratman, V.L., and Fedotov, A.E. (2002). Orotron: perspectives of advancing into submillimeter wavelength band. *Vacuum microwave electronics: Trans. Reviews*, p.p. 121-124.

Shestopalov, V.P. (1976). *Diffraction electronics*, Kharkiv University Publishers, Kharkiv.

Shestopalov, V.P. (1985). *Physical basis for millimeter- and submillimeter-wave equipment*, Naukova Dumka, Vol 1 (*Open-type structures*), Vol. 2 (*Sources, element basis – Radio systems*), Kyiv.

Shestopalov, V.P. (1991). *Diffraction radiation oscillators,* Naukova Dumka, Kyiv.

Shmatko, A.A (2008). *An electron-wave systems of millimeter wave range*, Vol. 1, KNU V.N. Karazina, Kharkov.

Smith, S.I., and Parcell, E.M. (1953).Visible light from localized surface charges moving across a grating. *Phys. Rev.*,Vol. 92, No 4, p.p. 1069-1073.

Sukhoruchko, O.N., Tkachenko, V.I., and Fisun, A.I. (2003). Modelling of elements of the air intake low-noise duct with parametric signal amplification. *Applied Radioelectronics*, Vol. 2, p.p. 163-167.

Valitov, R.A., Dyubko, S.F., Kamyshan, V.V et al. (1969). *Submillimeter-wave equipment*, Sov. Radio, Moscow.

Valitov, R.A., and Makarenko, B.I. (1984). *Measurements upon millimeter and submillimeter waves: Methods and equipment*, Radio i Svyaz, Moscow.

Vorobyov G.S. Pushkarev K.A.and Tsvyk A.I. (1997). Numerical analysis of shielding properties of diffraction grating excited by electron beam radiation on metal-dielectric structures. *Radiotehnika I Elektronika,* Vol.42, №2, p.p. 738-740.

Vorobyov G.S., Petrovsky M.V., Zhurba V.O., Ruban A.I., Belous O.I., and Fisun A.I. (2007). Perspectives of application of new modifications of resonant quasi-optical structures in EHF equipment and electronics. *Telecommunications and Radio Engineering,* Vol.66, Issue 20, p.p. 1839-1862.

Weinstein, L.A. (1966). *Open resonators and open waveguides*, Sov. Radio, Moscow.

Weinstein, L.A., and Solntsev, V.A. (1973). *Lectures on microwave electronics*, Sov. Radio, Moscow.

Weinstein, L.A. (1995). *Theory of diffraction. Microwave electronics*, Radio i Svyaz, Moscow.

Electromagnetic Waves

Edited by Prof. Vitaliy Zhurbenko

This book is dedicated to various aspects of electromagnetic wave theory and its applications in science and technology. The covered topics include the fundamental physics of electromagnetic waves, theory of electromagnetic wave propagation and scattering, methods of computational analysis, material characterization, electromagnetic properties of plasma, analysis and applications of periodic structures and waveguide components, and finally, the biological effects and medical applications of electromagnetic fields.

How to reference

In order to correctly reference this scholarly work, feel free to copy and paste the following:

Gennadij Vorobjov, Yulya Shulga and Vitaliy Zhurbenko (2011). Quasi-optical Systems Based on Periodic Structures, Electromagnetic Waves, Prof. Vitaliy Zhurbenko (Ed.), ISBN: 978-953-307-304-0, InTech, Available from: http://www.intechopen.com/books/electromagnetic-waves/quasi-optical-systems-based-on-periodic-structures

INTECH
open science | open minds